Friction and Wear Behavior of Basalt-Fabric-Reinforced/ Solid-Lubricant-Filled Phenolic Composites

Xinrui Zhang,[1,2] Xianqiang Pei,[1] Qihua Wang[1]

[1]*State Key Laboratory of Solid Lubrication, Lanzhou Institute of Chemical Physics, Chinese Academy of Sciences, Lanzhou 730000, China*
[2]*Graduate School, Chinese Academy of Sciences, Beijing 100039, China*

Received 22 April 2009; accepted 13 January 2010
DOI 10.1002/app.32085
Published online 12 May 2010 in Wiley InterScience (www.interscience.wiley.com).

ABSTRACT: To improve the tribological properties of basalt-fabric-reinforced phenolic composites, solid lubricants of MoS_2 and graphite were incorporated, and the tribological properties of the resulting basalt-fabric composites were investigated on a model ring-on-block test rig under dry sliding conditions. The effects of the filler content, load, and sliding time on the tribological behavior of the basalt-fabric composites were systematically examined. The morphologies of the worn surfaces and transfer films formed on the counterpart steel rings were analyzed by means of scanning electron microscopy. The experimental results reveal that the incorporation of MoS_2 significantly decreased the friction coefficient, whereas the inclusion of graphite improved the wear resistance remarkably. The results also indicate that the filled basalt-fabric composites seemed to be more suitable for friction materials serving under higher loads. The transfer films formed on the counterpart surfaces during the friction process made contributions to the reduction of the friction coefficient and wear rate of the basalt-fabric composites. © 2010 Wiley Periodicals, Inc. J Appl Polym Sci 117: 3428–3433, 2010

Key words: fibers; fillers; high performance polymers; reinforcement

INTRODUCTION

Polymer-based materials have been preferred in recent years over metal-based counterparts because of their low friction coefficient and ability to sustain loads. Particularly, polymer matrix composites reinforced with fibers have been widely accepted as tribological materials and have been used on components supposed to run without any external lubricants.[1,2] Fabric-reinforced polymer composites have high mechanical strengths in both the longitudinal and transverse directions; this has been considered as an advanced bearing liner material for tribological application in many high-tech industries, such as the aerospace, aviation, automobile industries, because of its low density, high strength, high modulus, excellent chemical stability, and anti-wear ability.[3,4] The friction and wear performance of fabric-reinforced composites is a complex phenomenon, which depends on the type of fabric and matrix, fiber volume fraction, fiber–matrix interfacial adhesion, orientation of warp and weft fibers with respect to sliding direction and sliding plane, and weaves of the fabric.[5] In fabric composites, matrices play the role of binding all of the fabric layers together, which plays a full part in improving the friction and wear properties of fabric composites. Moreover, the tribological behavior of fabric composites exhibits a strong dependence on the imposed friction conditions, for example, the sliding speed and applied load.[6–11]

Basalt fiber has better mechanical properties than E-glass fiber, is more widely available, and is cheaper than carbon fiber. In addition, basalt fiber is superior to glass and asbestos fiber because of the absence of carcinogenic effects, environmental cleanness, flexibility, good temperature resistance, and heating insulation properties.[12] Recently, basalt fiber has been used as a reinforcement material in a wide range of applications, such as heat-insulating materials and filtering materials. With the increasing application of basalt fibers, the investigations of basalt-fiber-reinforced polymer composites are being actively pursued. Currently, most studies are focused on the processes and mechanical and physical properties of basalt-fiber-reinforced composites. Wang et al.[13] studied the low-velocity impact properties of three-dimensional woven basalt/aramid hybrid composites and found that an interply hybrid composite had a higher ductility, lower peak load,

Correspondence to: Q. Wang (wangqh@lzb.ac.cn).
Contract grant sponsor: National Natural Science Foundation of China; contract grant number: 50805139.
Contract grant sponsor: Knowledge Innovative Engineering of the Chinese Academy of Sciences and Important Direction Project; contract grant number: KGCX3-SYW-205.

and higher specific energy absorption in both the warp and weft directions than an intraply hybrid composite. However, as a promising reinforcement material, the application of basalt fibers in tribological materials has been paid little attention. Experiments have revealed that it seems to be difficult to develop low-friction and high anti-wear polymer composites reinforced only with basalt fabric. So, it is imperative to seek effective ways to improve the tribological behavior of basalt-fabric composites (BFCs).

As it is known, some solid lubricants with lamellar structures are widely used to reduce both the friction coefficient and wear rate of some fabric composites or polymeric composites.[14–16] With this perspective in mind, MoS_2 and graphite were selected to fill the BFCs in the presence of phenolic adhesive resin. The objective of this study was to investigate and compare the effect of solid lubricants on the improvement of the tribological behavior of BFCs. It is expected that this study will bring a new application of basalt-fabric-reinforced polymer composites in dry sliding bearings.

EXPERIMENTAL

Materials

The basalt fabric used in this study was purchased from Weihai Guangwei Group Co., Ltd. (China). The properties of the basalt fabric are shown in Table I. The adhesive resin (phenolic resin) was provided by Shanghai Xing-Guang Chemical Plant (Shanghai, China). MoS_2 powders (<1.5 μm) and graphite powders (<1.5 μm) were provided by Shanghai Colloid Chemical Plant (Shanghai, China).

Preparation of the BFCs

The commercial basalt fabric was dipped in acetone for 24 h, then cleaned ultrasonically with acetone for 0.5 h, and dried before used. The solid lubricants were uniformly mixed with phenolic resin at proper mass fractions with the assistance of magnetic stirring. In this study, a dip-coating process was used to prepare the prepregs of the composites. First, the cleaned basalt fabric was dipped into a phenolic resin solution containing the solid lubricants and immersed in the solution ultrasonically for 10 min. Then, the fabric was put into an oven at 40°C to evaporate the solvent. A series of repeated dipping and coating of the basalt fabric was performed to allow the generation of the composite prepregs. The final BFCs were fabricated by means of a hot-press molding technique. The resulting prepreg was cut into long pieces of 50 × 30 mm^2 and put into the mold with plies orientations of [0°/0°]. The prepregs were compressed and heated to 180°C in the mold with intermittent deflation, and then, the pressure was held at 15 MPa for 240 min to allow full compression sintering. At the end of each run, the resulting specimens were cooled with the stove in air and then cut into preset sizes for friction and wear tests.

TABLE I
Properties of the Basalt Fabric

Basalt fabric	Plain
Type	264 tex
Ends per inch	4.9 filaments/10 mm
Picks per inch	4.9 filaments/10 mm
Density	492 g/m^2
Thickness	0.27 mm

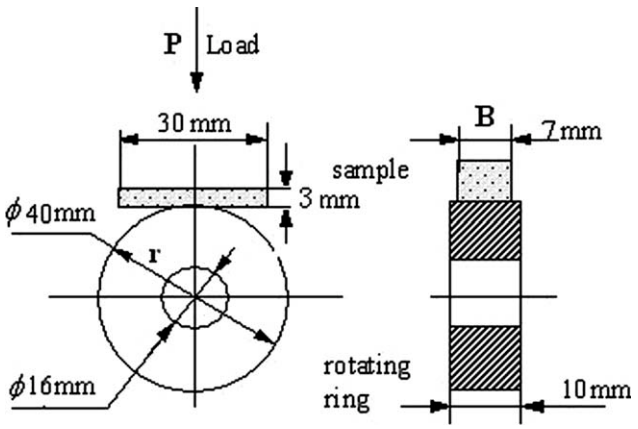

Figure 1 Contact schematic for the friction couple.

Friction and wear tests

The friction and wear tests were conducted on an M-2000 model friction and wear tester (made by Jinan Testing Machine Factory, Jinan, China). A schematic diagram of the block-on-ring type friction and wear tester used in this study is shown in Figure 1. The specimens for wear tests were machined with a geometry of 30 × 7 × 3 mm^3. Stainless GCr15 steel rings with a hardened and smoothly polished surface served as counterparts. The chemical composition of the GCr15 steel is given in Table II. Sliding was performed under ambient conditions over a period of 120 min at a sliding velocity of 0.431 m/s with a normal load ranging from 200 to 500 N. Before each test, the surfaces of the block specimens and counterpart rings were abraded with No. 1000 metallographic abrasive paper and then cleaned

TABLE II
Chemical Composition of the GCr15 Steel Ring

C (wt %)	Mn (wt %)	Si (wt %)	P (wt %)	S (wt %)	Cr (wt %)
0.95–1.05	0.25–0.45	0.15–0.35	≤0.025	≤0.025	1.40–1.65

with acetone-dipped cotton. During the friction process, the block specimen was static, and the steel ring slid against the block unidirectionally. The friction force was measured with a torque shaft equipped with strain gauges mounted on a vertical arm that carried the block, which was used to calculate the friction coefficient by taking into account the normal load applied. The width of wear tracks was measured with a reading microscope to an accuracy of 0.01 mm. Then, the specific wear rate (ω) of the specimen was calculated as follows:[17]

$$\omega = \frac{B}{L * P}\left[\frac{\pi r^2}{180}\arcsin\left(\frac{b}{2r}\right) - \frac{b}{2r}\sqrt{r^2 - \frac{b^2}{2}}\right]\left(\frac{\mathrm{mm}^3}{\mathrm{N}\cdot\mathrm{m}}\right)$$

where B is the width of the specimen (mm), r is the semidiameter of the stainless steel ring (mm), b is the width of the wear trace (mm), L is the sliding distance (m), and P is the load (N). In this study, three replicated wear results were averaged and taken as the wear results.

Worn surface analysis

The morphologies of the worn surfaces and transfer films formed on the counterpart steel rings were analyzed on a JSM-5600LV scanning electron microscope (Tokyo, Japan). To increase the resolution for scanning electron microscopy (SEM) observation, the tested composite specimens were plated with gold to render them electrically conductive.

RESULTS AND DISCUSSION

Tribological properties of the BFCs

In Figure 2, the friction coefficient and wear rate of the MoS_2-filled BFCs at a sliding speed of 0.431 m/s under 200 N are plotted versus the MoS_2 mass content. The friction coefficient and wear rate of the unfilled basalt fabric were relatively high. When a lower content of 5 wt % MoS_2 was incorporated, the friction coefficient and wear rate of the composite decreased slightly. With increasing MoS_2 content up to 15 wt %, the friction coefficient and wear rate of the composites sharply decreased, after which both of them increased. So, the optimal MoS_2 content was recommended to be 15 wt %, with the friction reduction and anti-wear ability of the composites considered.

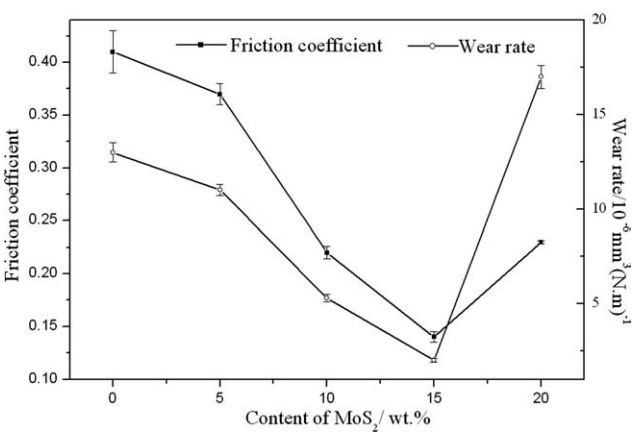

Figure 2 Variation of the friction coefficient and wear rate with various MoS_2 contents for the MoS_2-filled BFCs.

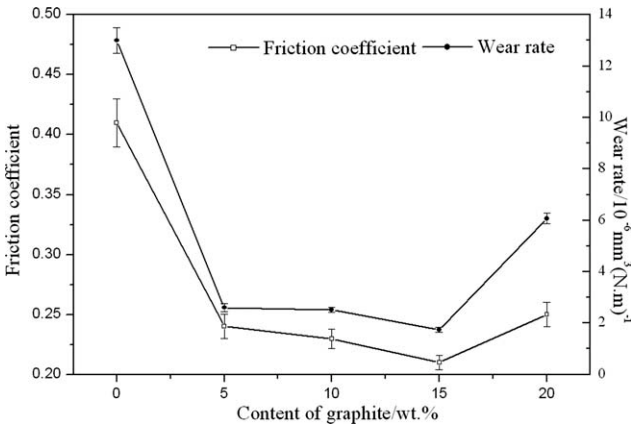

Figure 3 Variation of the friction coefficient and wear rate with various graphite contents for the graphite-filled BFCs.

Figure 3 shows the friction coefficient and wear rate of BFCs with various graphite contents at a sliding speed of 0.431 m/s under 200 N. It was clear that graphite contributed remarkably to the improvement of the friction and wear behavior of the BFCs. As shown, there was a significant reduction in the friction coefficient and wear rate of the composites at a graphite content as low as 5 wt %. With increasing graphite concentration, the declining trend became gentle. In the tested system, with regard to the friction coefficient and wear rate, the optimum content of graphite was about 15 wt %. Further addition of graphite impaired the friction reduction and anti-wear abilities of the composites, which may have been due to the fact that excessive graphite tended to conglomerate and led to lower uniformity of the system and, thus, reduced the anti-wear ability of the composites.

On the basis of these results, 15 wt % MoS_2 and graphite-filled BFCs were chosen to study the effects of the load on the friction and wear behavior of the BFCs. For comparison, the friction coefficient and wear rate of the unfilled BFCs are plotted in Figure 4 as a function of the load. Both the friction coefficient and wear rate of the unfilled BFCs increased with increasing load up to 300 N. This may have been due to the fact that more basalt fabrics dropped out from the phenolic matrix under higher loads (this was supported by SEM, as discussed in a subsequent section),

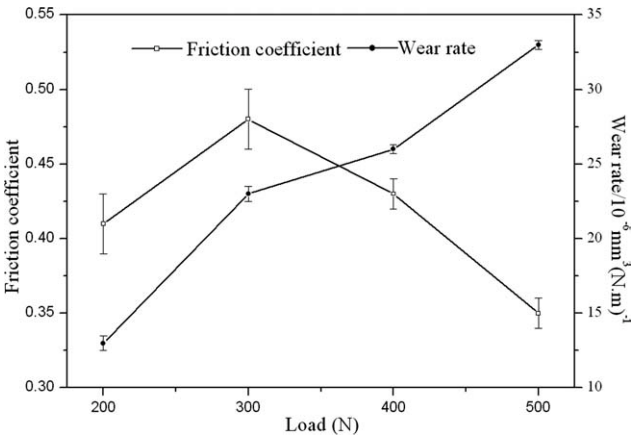

Figure 4 Variation of the friction coefficient and wear rate with the load for the pure BFCs.

which led to a severe abrasive wear and resulted in a higher friction coefficient and wear rate. When the load was beyond the previously mentioned range, the friction coefficient decreased drastically because of the micromelting and mechanical deterioration caused by friction heat under the higher load. Meanwhile, the wear rate of the unfilled BFCs increased with increasing load from 300 to 500 N. With an increase in load, the subsequent flash temperature increased and led to the following: the fiber–matrix adhesion deteriorated, and pulling out or peeling off of pulverized basalt fibers from the matrix became easy; hence, wear increased with increasing load.

Variations of the friction and wear behavior of the BFCs filled with 15 wt % graphite and MoS_2 with load are shown in Figure 5. Both the friction coefficient and wear rate of the filled BFCs decreased monotonically with increasing load. When the applied load increased, some big particle-shaped or flaky debris in the worn surface was crushed or sheared into smaller particles or thinner flakes and acted as lubricants. Concomitantly, the newly formed debris came into being as a more integrated but thinner film on the worn surface, and as a result, the smaller debris and more integrated but thinner film on the worn surface brought about smaller coefficients of friction because of the decreased degree of two-body abrasive wear.[18] Moreover, the transfer film easily formed because of the increase in adhesive force between the film and counterpart. The self-lubricating ability of the polymer composites largely depended on the formation of the transfer film on the sliding counterface, which further controlled the sliding performance. With the formation of a relatively uniform and coherent transfer film, subsequent sliding occurred between the surface of the BFCs and the transfer film. Consequently, a lower friction coefficient and wear rate were reached.

To illustrate the wear mechanism of the pure and filled BFCs, Figure 6 presents the typical evolutions of friction coefficients of 15 wt % MoS_2 and graphite-filled BFCs as a function of sliding time at 0.431 m/s under different loads. The friction process could be divided into two distinct stages: one was the running-in period, and the other was the steady-state period. It took a few minutes to transition from the running-in period to the steady-state period. The friction coefficient in the running-in period was much higher than that in the steady-state period. Moreover, the running-in period shortened, and the friction coefficient obviously decreased with increasing load, which was in full agreement with results presented previously. With increasing applied load, the transfer films was easily formed because of the increase in adhesive force between the film and counterpart. When the formation and peeling of the transfer films came to a balance, the friction coefficient became stable, which agreed well with the noted transition from high friction to low friction and separation between high wear in the running-in period and low wear in the steady-state period.

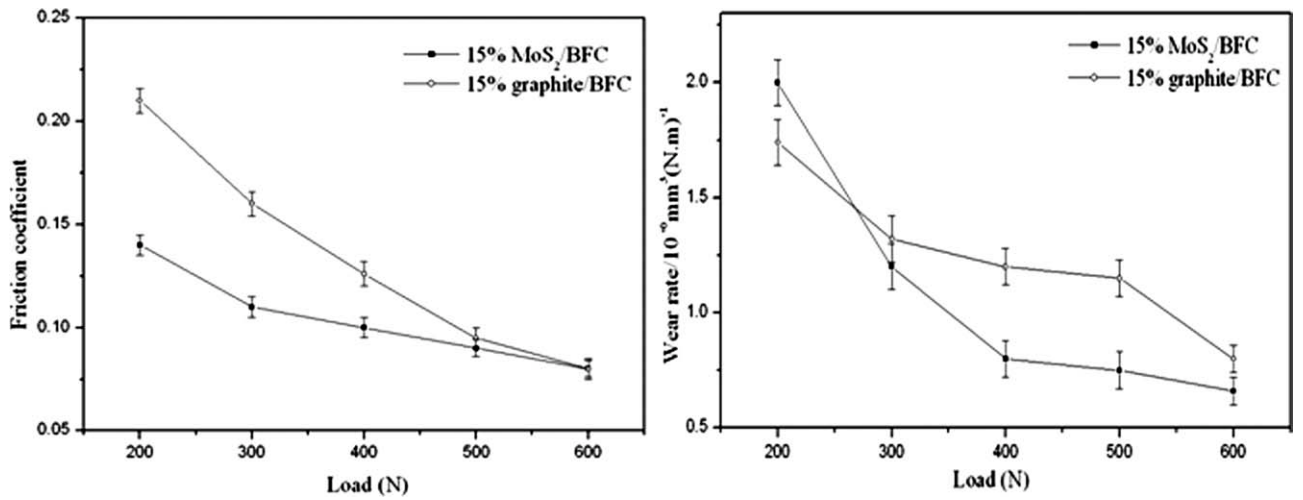

Figure 5 Variation of the friction coefficient and wear rate with the load for the MoS_2- and graphite-filled BFCs.

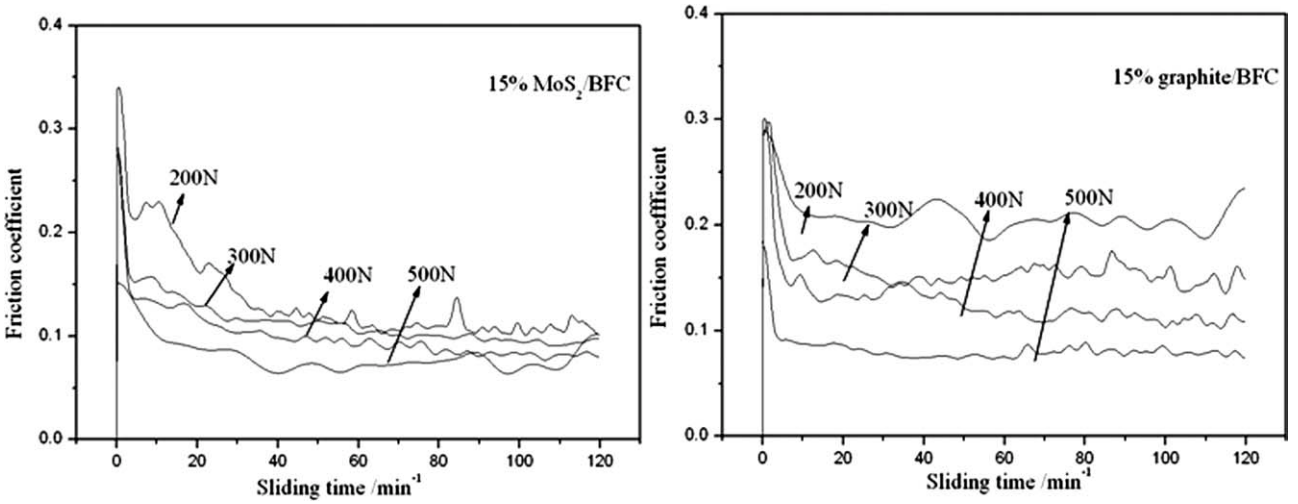

Figure 6 Effect of the sliding time on the friction and wear rate of the MoS_2- and graphite-filled BFCs (0.431 m/s, 200 N).

SEM analysis

Figure 7 shows the SEM morphologies of the worn surfaces of the BFCs and the transfer films formed on the GCr15 steel surfaces at a sliding speed of 0.431 m/s under 200 N. A few basalt fibers were pulled out and cut from the pure BFCs, which resulted in a slight abrasive wear [Fig. 7(a)]. Contrary to the unfilled BFC, the worn surface of the BFCs filled with 15 wt % MoS_2 and graphite was relatively smooth, and the pulling out and exposure of the basalt fibers was abated [Fig. 7(b,c)]. In particular, the worn surface of the 15 wt % MoS_2 filled BFCs was the smoothest, and little sign of basalt fiber damage was seen [Fig. 7(c)], which conformed to the best wear resistance of the composite. Accordingly, the morphologies of the corresponding transfer films were consistent with the wear resistance of the composites. For the pure basalt fiber composites, the transfer film formed on the counterpart steel ring appeared to be thick and discontinuous [Fig. 7(d)]; this corresponded to the poor wear resistance of this composite. On the contrary, comparatively thinner and homogeneous transfer films were formed on the counterpart surface friction against 15 wt % graphite and MoS_2 filled BFCs [Fig. 7(e,f)], which promised to provide better friction and wear behavior.

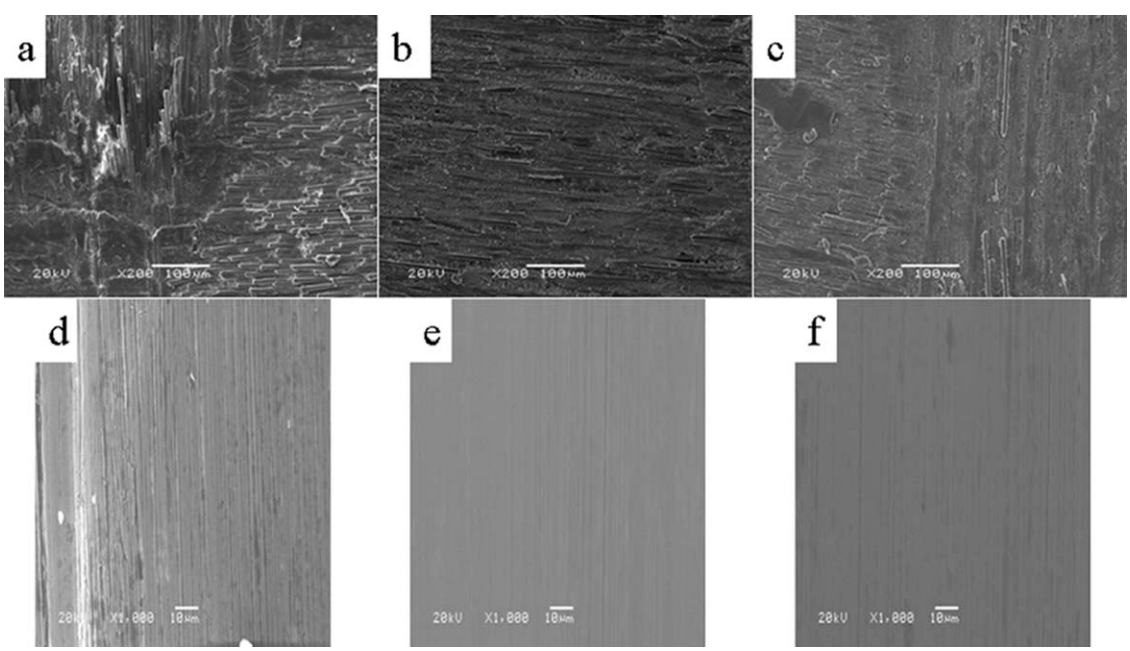

Figure 7 SEM morphologies of the worn surfaces and transfer films of the BFCs: (a) pure BFC, (b) 15% MoS_2/BFC, (c) 15% graphite/BFC, (d) transfer film of the pure BFC, (e) transfer film of the 15% MoS_2/BFC, and (f) transfer film of the 15% graphite/BFC.

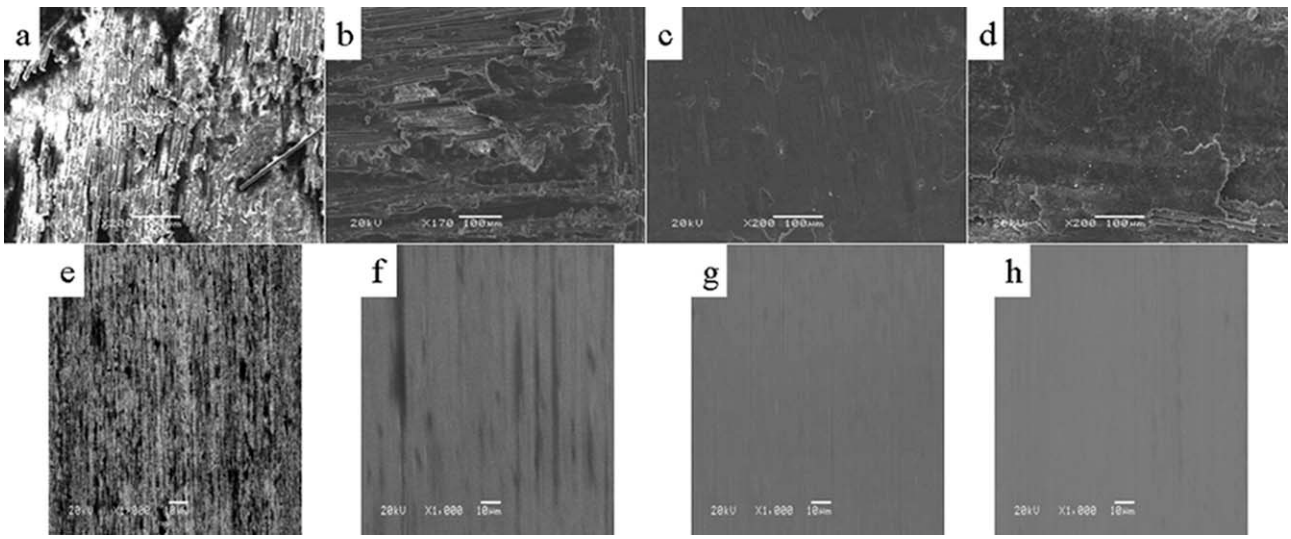

Figure 8 SEM morphologies of the worn surfaces and transfer films of the BFC composites sliding under different loads: (a) pure BFC at 300 N, (b) pure BFC at 500 N, (c) 15% MoS_2/BFC at 500 N, (d) 15% graphite/BFC at 500 N, (e) transfer film of the pure BFC at 300 N, (f) transfer film of the pure BFC at 500 N, (g) transfer film of the 15% MoS_2/BFC at 500 N, and (h) transfer film of the 15% graphite/BFC at 500 N.

When the load increased up to 300 N, the worn surface of the unfilled BFCs became more rough and was characterized by many pullings out and the exposure of the basalt fibers [Fig. 8(a)], which indicated that the unfilled BFCs experienced severe peeling off. The dropout of the basalt fibers from the phenolic matrix led to severe abrasive wear, which resulted in the removal of material through a combination ploughing/cutting effect. The transfer film [Fig. 8(e)] was rough, inhomogeneous, and discontinuous. Under a load of 500 N, the unfilled BFCs might have experienced micromelting, and many signs of peeling were also seen on the worn surface [Fig. 8(b)]. Under a higher load, a great deal of friction heat may have been produced, and the molecular chain of the phenolic matrix was relaxed, after which the phenolic matrix could be transferred to the counterpart surface more easily. The transfer film [Fig. 8(f)] was smoother but still not uniform, which resulted in a lower friction coefficient. As for the worn surfaces of 15 wt % MoS_2 or graphite-filled BFCs, the pulling out and exposure of basalt fibers became mild [Fig. 8(c,d)]. The corresponding transfer films [Fig. 8(g,h)] became thinner, continuous, and more coherent. It was just the transfer film that was responsible for the improved friction and wear behavior of the BFCs.

CONCLUSIONS

A systematic investigation of the tribological properties of BFCs was carried out in this study. The following conclusions were made:

1. An appropriate content of solid lubricants improved the tribological properties of the BFCs greatly. For the best combination of friction coefficient and wear rate, an optimal mass content of MoS_2 and graphite in the phenolic resin appeared to be 15%.
2. The differences in the friction and wear properties of the BFCs were closely related to the sliding conditions, such as load. The research results show that 15 wt % MoS_2 and graphite-filled BFCs exhibited better tribological properties under a higher load.

References

1. Biswas, S. K.; Kalyani, V. Wear 1992, 158, 193.
2. Wang, Y. Q.; Li, J. Mater Sci Eng A 1999, 266, 155.
3. Tercan, M.; Asi, O.; Aktas, A. Compos Struct 2007, 78, 392.
4. Lua, J. Compos A 2007, 38, 1019.
5. Bijwe, J.; Rattan, R.; Fahim, M. Tribol Int 2007, 40, 844.
6. Lu, Z. P.; Friedrich, K. Wear 1995, 181, 624.
7. Bassani, R.; Levita, G.; Meozzi, M.; Palla, G. Wear 2001, 247, 125.
8. Myshkin, N. K.; Petrokovets, M. I.; Kovalev, A. V. Tribol Int 2005, 38, 910.
9. Flom, D. G.; Porile, N. T. Nature 1955, 175, 682.
10. Flom, D. G.; Porile, N. T. J Appl Phys 1955, 26, 1080.
11. Milz, W. C.; Sargent, L. E. Lubr Eng 1955, 11, 313.
12. Kuryaeva, R. G.; Kirkinskii, V. A. Phys Chem Miner 1997, 25, 48.
13. Wang, X.; Hu, B.; Feng, Y.; Liang, F.; Mo, J. Compos Sci Technol 2008, 68, 444.
14. Khedkar, J.; Negulescu, I.; Meletis, E. I. Wear 2002, 252, 361.
15. Cenna, A. A.; Dastoor, P.; Beehag, A. J Mater Sci 2001, 36, 891.
16. Bahadur, S. Wear 2000, 245, 92.
17. Cai, H.; Yan, F. Y.; Xue, Q. J.; Liu, W. M. Polym Test 2003, 22, 875.
18. Friedrich, K.; Flock, J.; Varadi, K.; Neder, Z. Wear 2001, 251, 1202.